CLM - P 475

CLM - P 475

UKAEA RESEARCH GROUP

Preprint

LASER LIGHT SCATTERING AS A METHOD FOR MEASURING THE MAGNETIC FIELD DIRECTION IN A PLASMA

P G CAROLAN

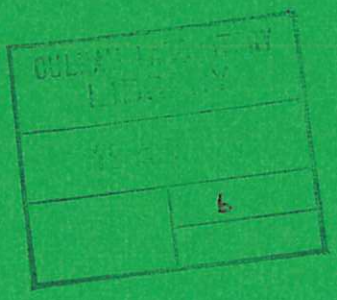

CULHAM LABORATORY
Abingdon Oxfordshire

1977

CLM-P 475

LASER LIGHT SCATTERING AS A METHOD FOR MEASURING THE MAGNETIC FIELD DIRECTION IN A PLASMA

P G Carolan

Culham Laboratory, Abingdon, Oxon, OX14 3DB, UK
(Euratom/UKAEA Fusion Association)

ABSTRACT

The spectrum of light scattered by a plasma in a magnetic field consists of a sequence of peaks if the scattering vector $\vec{k}$ is almost perpendicular to the magnetic field $\vec{B}$. Serious smearing of the peaks occurs when $2kv_e \cos\phi \geq \omega_{ce}$ where ϕ is the angle between $\vec{k}$ and $\vec{B}$. Hence the scattered light will exhibit modulation only within a thin angular wedge. The angular location of this wedge can be determined by using a Fabry-Perot or a Michelson interferometer and from this the direction of the magnetic field can be determined. A generalised treatment is presented to allow for the interpretation of experimental results from any light scattering arrangement or plasma field configuration. The limits imposed on this diagnostic technique, such as the laser beam divergence and field uniformity, are also derived. For a representative Tokamak plasma of B_{tor} = 3 T, B_{pol} = 0.3T and T_e = 1 keV, the poloidal field must be uniform within 0.015T in the scattering volume for 30^o scattering by a ruby laser beam whose divergence must be less than 3 mrad to obtain an accuracy of about 5% in the determination of the ratio B_{pol}/B_{tor}.

(Submitted for publication in Plasma Physics)

November 1976

LIST OF SYMBOLS

$\vec{B}_\phi$	toroidal magnetic field
$\vec{B}_\theta$	poloidal magnetic field
c	speed of light
- e	electron charge
F	Fabry-Perot finesse
$\vec{k}$	scattering or differential wave vector
$\vec{k}_o$	incident wave vector
$\vec{k}_s$	scattered wave vector
OL	laser axis
OS	collection optics axis
M	telescope magnification
n_e	electron density
q	image tube quantum efficiency
r_b	laser beam radius
r_e	classical radius of an electron
T_e	electron temperature
T_R	collection optics transmission factor
v_e	electron thermal velocity
x,y,z	basic frame of reference whose origin is at the scattering volume and where
$\hat{e}_y$	unit vector parallel to torus major axis
$\hat{e}_z$	$\equiv \hat{e}_\phi$, unit vector in the toroidal direction
$\hat{e}_x$	$\equiv \hat{e}_y \times \hat{e}_z$
W	laser beam energy
β	angle between $\vec{B}_\theta$ and laser beam axis
γ_o	laser beam divergence at the scattering volume
γ_s	half apex angle of collection cone of scattered light directions
δ_o, δ_s	inclination angle of laser beam, collection cone to torus major axis
ε	angle between $\vec{B}$ and $\vec{B}_\theta$

θ	single value scattering angle
Θ	angle between laser axis and axis of collection optics
λ_o	laser wavelength
μ_o, μ_s	laser beam, collection cone azimuthal angle
$\Delta\mu_s$	half azimuthal angle width of scattered light which exhibits modulation
ξ_o, ξ_s	laser beam axis, collection cone axis azimuthal angle about torus major axis direction
ϕ	angle between $\vec{k}$ and $\vec{B}$
χ_o, χ_s	apex angle in laser beam, collected scattered light
χ_{SMN}	minimum collection cone apex angle required to detect magnetic modulated light
χ_{OMX}	maximum laser beam divergence (in the plasma), permitted to retain highest accuracy in field direction determination
ω_{ce}	electron gyro frequency
$\delta\Omega$	solid angle subtended by partial interference fringe
$\Delta\Omega$	solid angle subtended by Fabry-Perot interference ring

1. INTRODUCTION

The technique of laser light scattering has been successfully employed in measuring the intensity of a plasma magnetic field (Evans & Carolan (1970), Kellerer (1970) and Ludwig & Mahn (1971)). The direction of the magnetic fields in these experiments was known fairly accurately and the mean weighted differential scattering vector (Carolan & Evans (1971a), Carolan & Evans (1971b)), $\vec{k}_{av}$, was arranged perpendicular to this direction. When both the electron Larmor radius and the Debye length greatly exceed the scattering scale length, k_{av}^{-1}, the scattered spectrum should exhibit modulation with peaks located at integer multiples of the electron gyro frequency ω_{ce}. The width of the individual peaks is approximately (Carolan & Evans (1971a), Meyer & Leclert (1972)) $2kv_e \cos \phi_{av}$, where $v_e = \sqrt{2KT_e/m_e}$ and ϕ_{av} is the angle between $\vec{k}_{av}$ and $\vec{B}$. When this width exceeds the peak spacing serious smearing occurs.

There have been several suggestions (Murakami & Clarke (1971), Perkins (1970) and Sheffield (1972)) put forward on how the method might be extended to measure the magnetic field direction. They all take advantage of the sensitive dependency, especially at high electron temperatures, of the modulated spectrum on aligning $\vec{k}$ perpendicular to $\vec{B}$. Sheffield made the novel proposal by which the directions of scattered light which gave the deepest modulation could be measured in one shot. These directions yield the values of the scattering wave vectors, $\vec{k}$, which satisfy the relationship $\vec{k}.\vec{B} = 0$. For the scattering geometry suggested it was then a simple matter to determine the field direction. A typical light scattering arrangement to measure the magnetic field direction in a Tokamak plasma is shown in Figure 1. Suppose, for simplicity, that the laser beam is perpendicular to the poloidal field. The scattered light with the highest modulation will then be directed along a plane perpendicular to $\vec{B}$. The angular location of this plane may be found by the observation of partial interference fringes from a Fabry-Perot (or Michelson) whose free spectral range matches the electron gyro frequency.

In this paper the basic principles of Sheffield's proposal is generalized to

include the whole range of scattering arrangements and magnetic field configurations. Also included are the safeguards which must be taken to limit the effect of real experimental conditions, such as magnetic field gradients, which reduce the quality of the diagnostic. Using the generalized treatment comparisons are made between different scattering arrangements e.g. at 90^{o} scattering more accurate determinations of the field direction are possible but proper matching of the interferometer to the peak spacing is more difficult.

Since all possible scattering geometries are included in this treatment, the effects of laser beam and collection optics misalignments are implicitly considered.

2. EXPRESSION OF $\vec{B}$ AND $\vec{k}$ IN COMPONENT FORM FOR A GENERAL SCATTERING ARRANGEMENT

In a successful experiment to measure the magnetic field direction, by the scattering of laser light, the directions of such scattered light that exhibits 'magnetic modulation' will constitute the basic raw data. In these directions, the scattering wave vector, $\vec{k}$, will be perpendicular to the magnetic field, $\vec{B}$, (i.e. $\vec{k}.\vec{B} = 0$) and the scattered spectra will consist of peaks separated by the electron gyro frequency, ω_{ce}, and contained within a Gaussian envelope of width $2kv_{e}$. Given the angular coordinates of the laser beam it then remains to determine the magnetic field direction from the experimental data.

A general treatment is presented here to provide for all possible laser scattering arrangements, including misalignments, and magnetic field configurations. The basic method adopted is to describe angular coordinates in frames of reference most convenient from the experimentalist's point of view and, then, transform these directions to a basic frame of reference and by imposing the alignment condition, $\vec{k}.\vec{B} = 0$, determine the magnetic field direction.

In Figure 2(a) is illustrated the toroidal and poloidal magnetic fields in the plasma, the axis OL of the laser beam and the axis OS of the collected cone of scattered light. The point O is a representative point in the scattering

volume. The basic x,y,z coordinate system is determined by the major axis and toroidal directions and the scattering volume as in Figure 2(b). The vectors $\vec{B}_\phi$ and $\vec{B}_\theta$ are the plasma toroidal and poloidal magnetic fields respectively. Expressing $\vec{B}$ in component from we have

$$\vec{B} = \begin{pmatrix} -B_\theta \sin\beta \\ B_\theta \cos\beta \\ B_\phi \end{pmatrix}_{x,y,z} \tag{1}$$

where β is the angle between $\vec{B}_\theta$ and the y axis.

Although arbitrary laser beam and collected scattered light directions are considered throughout the derivations following, the scattering arrangement is presented in a more restricted range in Figure 3 to improve the conceptual clarity of the method. (The general representation is presented in Figures A.1 and A.2 in the Appendix). Using conical coordinate systems, a particular laser wave vector and scattered light vector is described by $\vec{k}_o = (k_o, \chi_o, \mu_o)$ and $\vec{k}_s = (k_o, \chi_s, \mu_s)$ respectively, where χ_o and χ_s are apex angles and μ_o and μ_s are azimuthal angles. (It is assumed here that $|\vec{k}_s| = |\vec{k}_o| = k_o$ for small Doppler shifts). In order to determine the scattering wave vector, given by

$$\vec{k} = \vec{k}_s - \vec{k}_o \tag{2}$$

it is necessary to express the components of $\vec{k}_o$ and $\vec{k}_s$ in a common coordinate system. The required transformation matrices for the defined x,y,z coordinate system are given in the Appendix. At this point it is convenient to describe a misalignment factor by

$$f_{al}\left(\vec{B}, \vec{k}_o, \vec{k}_s\right) = \vec{B}.\vec{k} \quad . \tag{3}$$

The scattered light will exhibit maximum modulation when the misalignment factor is zero. When the conical coordinates of the modulated scattered light are known we can then determine the ratio B_θ/B_ϕ from

$$\frac{B_\theta}{B_\phi} = \frac{k_z}{k_x \operatorname{Sin}\beta - k_y \operatorname{Cos}\beta} \quad . \tag{4}$$

Since the angle β is in general not known, it is necessary to find experimentally

at least two directions of the scattered light that exhibits maximum 'magnetic modulation' to determine the magnetic field direction.

To bring out the essential features of the points made above, consider the case where the plasma is illuminated by a perfectly parallel laser beam which is parallel to the torus major axis and is at normal incidence to the poloidal field (i.e. the angle β of Figure 2 (a) is 90^{o}) in the region of the scattering volume.

Under these conditions the geometrical analysis can be simplified a great deal. In Figure 4 the centre of the sphere is a representative point in the scattering volume; the laser beam is the axis of the sphere whose radius is k_o. Therefore all scattering directions can be represented by points on the sphere's surface. So circular areas on the surface represent cones of scattered wave vectors for various scattering geometries. The angle, δ_s, between the cone axis and the laser beam, can be represented here by the lines of latitude. A particular scattering wave vector, $\vec{k}$, is that obtained by joining the 'north pole' point to the surface point corresponding to the scattered direction considered. The plane containing the vectors $\vec{k}_o$ and $\vec{k}$ will then intersect the surface of the sphere along a line of longitude containing this point. For the line of longitude given by $\eta = 0$, the corresponding plane will be perpendicular to the plane of the diagram. As represented in Figure 4, this plane is perpendicular to $\vec{B}_\phi$. If the poloidal field were zero, then, in this case all scattered wave vectors in the $\eta = 0$ plane would satisfy the perpendicularity condition of $\vec{B}.\vec{k} = 0$, and so magnetic modulation in the scattered spectra would be observed. However, for a finite poloidal field the relevant plane will be represented by the longitudinal line $\eta = \varepsilon$ where ε is the angle between $\vec{B}$ and $\vec{B}_\phi$ (cf. Figure 4 where, in this case, the poloidal field lies perpendicular to the plane of the diagram). When the cone axis of the collected scattered light lies in the $\eta = 0$ plane, (e.g. the geometry depicted in Figure 3) the azimuthal angle, μ_s', at which modulation will be observed, can be shown to be

$$\mu_s' = \sin^{-1}\left\{ \frac{B_\theta \sin \delta_s}{B_\phi \tan \chi_s \, (1+\alpha)^{\frac{1}{2}}} \right\} - \tan^{-1} \alpha \qquad (5)$$

where $$\alpha = \frac{B_\theta}{B_\phi} \cos \delta_s \quad . \qquad (6)$$

3. DETERMINATION OF THE LIMITING FACTORS GOVERNING THE OBSERVATION OF MAGNETIC MODULATION

3.1 Angular considerations

(a) Collected scattered light

Serious smearing will occur in the modulation of the scattered spectrum when the width of the individual peaks approaches the spacing of the peaks. When

$$2 k v_e \cos \phi = \omega_{ce} \qquad (7)$$

where ϕ is the angle between $\vec{k}$ and $\vec{B}$, the degree of modulation will be less than 30%. For the purposes of this paper, this will be considered to be at the limit of resolution. Suppose that maximum modulation is observed at a certain azimuthal angle, μ_s', in a cone of scattered light. We will now determine the change, $\Delta\mu_s$, in the azimuthal angle for which modulation will disappear.

We have for the misalignment factor

$$f_{al} (\mu_s') = 0 \qquad (8)$$

and from Eqns. (3) and (7)

$$f_{al} (\mu_s' + \Delta\mu_s) = \vec{k}.\vec{B} = \frac{B \omega_{ce}}{2 v_e} \qquad (9)$$

where B is in teslas. For magnetic fields and electron temperatures of interest the quantity $\Delta\mu_s$ can be considered to be a differential so from Eqns. (8) and (9) we can write

$$f_{al} (\mu_s' + \Delta\mu_s) \simeq \frac{\partial}{\partial \mu_s} f_{al} (\mu_s') \, \Delta\mu_s = \frac{B\omega_{ce}}{2v_e} \quad . \qquad (10)$$

We then get

$$\Delta\mu_s = \frac{B}{B_\phi} \cdot \frac{\omega_{ce}}{2v_e\, k_o \sin\chi_s\, g_s} \quad . \qquad (11)$$

(The derivation of Exp. (11) and the definition of g_s are given in the Appendix). Obviously the smaller the quantity $\Delta\mu_s$ the more accurate the magnetic field direction can be determined. Since $\Delta\mu_s$ has approximately an inverse dependency on sin χ_s the field direction can be measured more accurately for large values of cone apex angles, χ_s. For the restrictive scattering arrangement discussed in the previous section, and where $B_\theta/B_\phi << 1$, we have the approximate numerical expression

$$\Delta\mu_s \approx 1.4 \times 10^6 \frac{B\lambda_o}{T_e^{\frac{1}{2}} \sin\chi_s} \text{ degrees} \qquad (12)$$

where λ_o is the laser wavelength in metres and T_e the electron temperature in eV. As the ratio B_θ/B_ϕ increases, the plane containing the modulated light will increase its inclination angle to the plane defined by the laser axis and the torus axis. If the collected cone axis of scattered light lies in the latter plane it can be easily shown that to collect the modulated scattered light a minimum apex angle, χ_{SMN}, is required where

$$\chi_{SMN} \approx \tan^{-1}\left(\frac{B_\theta}{B_\phi} \sin\delta_s\right) \quad . \qquad (13)$$

(b) Laser beam divergence

In the scattering experiments performed to measure the magnetic field intensity by laser light scattering, it was clearly seen (Carolan & Evans (1971b)) to be advantageous to have a laser beam of relatively large divergence to assist in the alignment problems. The opposite applies to magnetic field direction measurements where it is important to enhance the effect of 'misalignment', between the scattering wave vector, $\vec{k}$, and the plane perpendicular to $\vec{B}$, and so increase the experimental accuracy.

For any particular direction of scattered light, there will always be a range of corresponding scattering wave vector directions due to the finite divergence of the laser beam illuminating the plasma. Consider the case where a range of scattered light directions manifest maximum modulation for a single incident wave vector in the axial direction of the laser beam. As a figure of merit we will require that the beam divergence be sufficiently small so that the degree of modulation of the scattered light spectrum, arising from any other incident wave vector within the laser beam cone, be always greater than about 30% (i.e. $2kv_e \cos \phi \lesssim \omega_{ce}$). The maximum beam divergence, χ_{OMX}, can be shown (cf. Appendix) to be

$$\chi_{OMX} \approx \frac{\omega_{ce}}{2k_o v_e}$$

or numerically

$$\chi_{OMX} \approx 2.36 \times 10^4 \frac{\lambda_o . B}{T_e^{\frac{1}{2}}} \text{ radians}$$

where $\frac{B_\theta}{B_\phi} << 1$ (Tokamak plasmas).

When the beam divergence exceeds χ_{OMX} the increment, $\Delta\mu_s$, of azimuth angle wherein magnetic modulation is observed, increases and thus the accuracy in determining the field direction is reduced.

3.2 Magnetic field uniformity

Suppose for a particular scattering direction, maximum magnetic modulation obtains for the central field values B_ϕ and B_θ of the scattering volume. Since the magnetic field intensity and direction can be expected to vary in any finite volume of plasma, the scattered light, originating from different points within the scattering volume, will exhibit different peak spacings and degrees of modulation. We will consider these two effects separately.

3.2(a) Uniformity of magnetic field directions

The magnetic field directions within a scattering volume will be contained within some cone in vector space. Suppose for the central field direction (i.e. the cone axis) a maximum degree of modulation will be observed in a particular scattering direction. Scattered light originating from other points will exhibit less modulation in this direction due to the increase in the misalignment between the plane perpendicular to $\vec{B}$ and the fixed $\vec{k}$ direction. The detected spectrum will be a composite one consisting of the weighted superposition of many spectra of different degrees of modulation in much the same way as described by Carolan & Evans (1971a). Eventually, for a relatively wide range of field directions the degree of modulation of the composite spectrum will be unacceptable. In the Tokamak context it is more meaningful to speak of the maximum range of toroidal and poloidal fields acceptable for a useful experiment. Using the same figure of merit described above and proceeding in a manner similar to that used in section 3.1(a) we obtain for all scattering arrangements a limit to the variation ΔB_ϕ and ΔB_θ of the toroidal and poloidal fields, given by

$$\left| \Delta B_\theta - \Delta B_\phi \cdot \frac{B_\theta}{B_\phi} \right| \leq \left| \frac{B\, B_\theta\, \omega_{ce}}{2 B_\phi\, k_z\, v_e} \right| \quad . \tag{14}$$

When the scattering arrangement is restricted as above it can be easily shown that for the most stringent B_θ/B_ϕ values we obtain

$$\left| \Delta B_\theta - \Delta B_\phi \cdot \frac{B_\theta}{B_\phi} \right| \leq \frac{B\omega_{ce}}{2k_o\, v_e\, (\cos\delta_s \sin\chi_s + \sin\delta_s \cos\chi_s)} \tag{15}$$

or numerically

$$\left| \Delta B_\theta - \Delta B_\phi \frac{B_\theta}{B_\phi} \right| \leq 2.36 \times 10^4 \frac{\lambda_o B^2}{T_e^{\frac{1}{2}} (\cos\delta_s \sin\chi_s + \sin\delta_s \cos\chi_s)} \quad . \tag{16}$$

For larger values of ΔB_θ and ΔB_ϕ loss of experimental accuracy ensues.

3.2(b) Uniformity of magnetic field intensity

In any finite scattering volume of a magnetized plasma the electrons will execute gyro orbits of different frequencies because of the finite range of magnetic field intensity. As a result, the 'magnetic modulation' scattered spectra generated will have slightly different peak spacings. The detection system will,of course, see only a weighted superposition of the scattered spectra. This spread of peak spacings is of little significance if only the first few peaks about the laser line are of interest, as was the case in the experiments performed to measure the field intensity. However, in high temperature, low density plasmas, it is important to utilize a large fraction of the scattered spectrum due to the unacceptable small number of photons per peak. In this case the limit of field variations is more stringent to ensure the spectral overlapping of high order peaks.

Suppose that there is a total field variation of ΔB, about the central field intensity B_o, within the scattering volume. We will assume that it is desirable to utilize all the light in the scattered spectra within the 1/e intensity points of the Gaussian envelope enclosing the peaks. In the vicinity of a frequency shift $n\omega_{ce}$ from the laser frequency, complete smearing out of the spectral peaks will occur when

$$n\omega_{ce}^{+} - n\omega_{ce}^{-} = \omega_{ce} \tag{17}$$

where

$$\omega_{ce}^{+} = \frac{e}{m}(B_o + \Delta B) \; ; \; \omega_{ce}^{-} = \frac{e}{m}(B_o - \Delta B) \; ; \; \omega_{ce} = \frac{e}{m} B_o \quad .$$

On substituting for the electron gyro frequencies in Eqn. (17) we find that in order to observe n peaks we require

$$\frac{\Delta B}{B_o} << \frac{1}{2n} \quad . \tag{18}$$

The peak order number at the 1/e intensity point is simply

$$n_{1/e} = \frac{kv_e}{\omega_{ce}} \quad . \tag{19}$$

So to collect the 85% of the total scattered light, contained within the 1/e intensity points, we require

$$\frac{\Delta B}{B_o} << \frac{\omega_{ce}}{2kv_e} \tag{20}$$

or numerically

$$\frac{\Delta B}{B_o} << 1.2 \times 10^4 \frac{\lambda_o B}{T_e^{\frac{1}{2}} \sin \theta_{av}/2} \tag{21}$$

where θ_{av} is the average scattering angle.

3.3 Accuracy of magnetic field direction determination

For a fixed value of apex angle, χ_s, in the scattered light, magnetic modulation for different values of B_θ/B_ϕ, will be observed at different azimuthal angles, μ_s'. The more sensitive μ_s' is to small changes in B_θ/B_ϕ, the more accurate field direction measurements can be made. The absolute accuracy is given, approximately, by

$$\Delta \left(\frac{B_\theta}{B_\phi}\right) = \Delta\mu_s \cdot \frac{\partial}{\partial\mu_s}\left(\frac{B_\theta}{B_\phi}\right) \tag{22}$$

where $\Delta\mu_s$ is obtained from Eqn.(12) and the derivative obtained from Eqn.(4). The derivative $\frac{\partial}{\partial\mu_s}\left(\frac{B_\theta}{B_\phi}\right)$ is plotted in Figure 5 as a function of δ_s for $B_\theta/B_\phi = 10\%$, $\chi_s = 8^o$ and $\beta = 90^o$. It can be seen immediately that more accurate B_θ/B_ϕ measurements can, in principle, be made at larger values of δ_s.

3.4 Interferometer and detection system

Most methods proposed to measure the magnetic field direction, by the scattering of laser light, rely on measuring the spectral profile of individual peaks in the scattered spectrum. However, the finite laser beam divergence and collection aperture in addition to the non-uniformity of the magnetic field in the scattering volume, affect substantially the peak profile. Unless the correct deconvolutions of the detected spectrum are used, the final result will be in error. Sheffield's proposal, on the other hand, would detect simultaneously the scattered light from a relatively wide range of angles,

and by identifying the scattering directions which exhibit maximum modulation the field direction can be determined. In what follows, we will consider the important features of the interferometer and detection system required for such an experiment.

The peak spacing in the modulated spectrum, for an incident ruby laser beam (at present the most attractive from the photodetection aspect), is given by

$$\Delta\lambda_M = .45 \text{ Å/tesla for } \lambda_o = 6943 \text{ Å} \quad . \tag{23}$$

Magnetic fields in the range of 2 to 5 teslas are typical of those used in plasma confinement machines, thus necessitating relatively fine resolution detection of the scattered spectrum. Amplitude division interferometers such as the Fabry-Perot and the Michelson can easily achieve this high resolution and both have a much higher light transmittance than the equivalent grating (Jacquinot (1954)). These interferometers behave as wavelength and angular filters, and so angular information in the light illuminating the interferometer is retained for monochromatic light or narrow lines separated in frequency by the free spectral range.

The Fabry-Perot and the Michelson mirror spacing (Katzenstein (1972)) is chosen to tune-in on the frequency of modulation of the spectrum by setting the free spectral range of the interferometer equal to the peak spacing on adjusting

$$d = \frac{\pi c}{\omega_{ce} \text{ Cos } \psi} \tag{24}$$

where d is the mirror spacing, c the velocity of light and ψ is the angular radius of an interference ring produced when the interferometer is illuminated by light of the laser wavelength. In this case the interference fringe patterns from all the peaks are superposed. This superposition technique makes more efficient use of the scattered light and may be critical in some scattering experiments on low density, high temperature plasmas. The modulated scattered light will be almost completely transmitted by the resonant Fabry-Perot when the incident angle, χ_s, equals ψ. However, the modulated light will be

contained only within a small increment, $2\Delta\mu_s$, of azimuth and, as a result, two bright partial interference fringes, instead of the usual rings, will be observed at azimuthal angles, μ_s', of scattered light where $\vec{k}.\vec{B} = 0$. These fringes constitute the raw data from which the field direction can be calculated. An attractive method of locating the angular positions, χ_s, μ_s, of the partial fringes has been suggested by Katzenstein (1972). This entails placing the photocathode of a gated image intensifier in the focal plane of either interferometer as illustrated in Figure 1.

Outside of the plane defined by the partial fringes, the scattered light will be featureless. Since the total light intensity is the same for both the modulated and unmodulated spectra, in the latter the light intensity at the peak frequencies will be relatively low. Consequently, as the interferometer is 'tuned-in' to the peak frequencies at the partial fringes, the average transmission of the interferometer will also be relatively low for unmodulated light which forms the background light to the bright partial fringes.

It is, of course, desirable to have high contrast fringes. We will now determine the fringe contrast factor as a function of the interferometer finesse, F.

The relative transmission $T(\omega)$ of a Fabry-Perot for an incident frequency, ω, is given by the Airy function (Born and Wolf (1959))

$$T(\omega) = \left[1 + \frac{4F^2}{\pi^2} \, \mathrm{Sin}^2 \left(\frac{\pi \omega}{\Delta\omega_{SR}} \right) \right]^{-1} \tag{25}$$

where $\Delta\omega_{SR}$ is the free spectral range and F is the finesse of the Fabry-Perot and given by

$$F = \frac{\pi\sqrt{R}}{1-R} \tag{26}$$

where R is the reflectivity of the plates.

The average transmission, $\tilde{T}$, is then obtained from

$$\tilde{T} = \int_{\omega}^{\omega+\Delta\omega_{SR}} \frac{T(\omega)}{\Delta\omega_{SR}} \, d\omega \tag{27}$$

It is a simple matter to show that Eqn (27) can be expressed by

$$\tilde{T} = \frac{1}{2\pi} \int_0^{2\pi} \frac{d\rho}{1 + \frac{4F^2}{\pi^2} \operatorname{Sin}^2 \frac{\rho}{2}} \tag{28}$$

where ρ is a free parameter. On evaluating the integral we get

$$\tilde{T} = \left(1 + \frac{4F^2}{\pi^2}\right)^{-\frac{1}{2}} . \tag{29}$$

Since the modulated light will be fully transmitted by the interferometer at the fringe positions we get for the fringe contrast factor, κ,

$$\kappa = (\tilde{T})^{-1} = \left(1 + \frac{4F^2}{\pi^2}\right)^{\frac{1}{2}} . \tag{30}$$

Alternatively, the dark spots of the interferometer pattern can be used where the modulated light is largely reflected by the interferometer. The relative transmission factor is obtained by simply taking the minimum value of the Airy function (Eqn 25) giving

$$T_{dark} = \left(1 + \frac{4F^2}{\pi^2}\right)^{-1} . \tag{31}$$

On comparing Eqn (31) with Eqn (29) we see that the dark spots of the interferometer pattern will have the same contrast factor as that of the fringes. Due to the small number of photoelectrons involved (cf. section 4) the bright fringes will give the more accurate determination of the field direction. From the transmission point of view the Michelson interferometer can be regarded as a low finesse Fabry-Perot with the consequent disadvantage of having a low contrast factor of the partial fringes. In what follows, therefore, we will concentrate on the Fabry-Perot (the approximate corresponding values for the Michelson may be obtained by setting F = 2).

It remains to calculate the solid angle subtended by the partial interference fringe. It can be easily shown that the solid angle, $\Delta\Omega$, subtended by a complete interference ring is given by

$$\Delta\Omega = \frac{\pi\lambda_o}{dF} \quad . \tag{32}$$

On substituting for the mirror spacing, d, we get

$$\Delta\Omega = \frac{\lambda_o\ \omega_{ce}}{cF} \quad . \tag{33}$$

The total solid angle, $\delta\Omega$, subtended by the partial fringe is then given by

$$\delta\Omega = \frac{\lambda_o\ \omega_{ce}\ \Delta\mu_s}{\pi cF} \quad . \tag{34}$$

Since in general the collection aperture will be large enough to illuminate several interference rings it is of advantage to use a telescope (cf. Figure 1) to illuminate only the central ring of the interference pattern and thereby increasing the light intensity. In this case we get

$$\delta\Omega = \frac{M^2\ \lambda_o\ \omega_{ce}\ \Delta\mu_s}{\pi cF} \tag{35}$$

where M is the telescope magnification factor.

3.5 Number of useful photoelectrons

As we shall see, the major difficulty that will be encountered in measuring the magnetic field direction by laser light scattering in a Tokamak plasma will be the small number of photoelectrons per partial interference fringe. It is therefore worthwhile determining the important parameters which limit this number and how they may be optimised.

The number of photons, Nph, scattered into a solid angle, $d\Omega$, is given by

$$Nph = \frac{W}{h\nu_o}\ r_e^2\ n_e\ L_S\ d\Omega \tag{36}$$

where W is the laser energy, ν_o the laser frequency, r_e classical electron radius, n_e the plasma electron density and L_S the scattering length defined by

$$L_S = \frac{V_S}{A_L} \tag{37}$$

where V_S is the scattering volume and A_L the area of the laser beam. The scattering volume is, by definition, the intersection volume of the laser beam

and the volume defined by the collection optics. The latter can be regarded as a cylinder when an amplitude division interferometer of the Fabry-Perot or Michelson is used as the dispersive instrument, due to the inherent symmetry about the optic axis. In this case the scattering volume is simply the intersection volume of two cylinders which can be shown to be

$$V_S = \frac{8\, r_1^{\,3}}{\sin\Theta} \int_o^1 (1-\rho^2)^{\frac{1}{2}} \left(\frac{r_2^{\,2}}{r_1^{\,2}} - \rho^2 \right)^{\frac{1}{2}} d\rho \qquad (38)$$

where r_1 and r_2 are the radii of the small and large cylinders respectively, Θ is the angle between the axes and ρ is a free parameter. The volume, V_S, can then be evaluated in terms of elliptic integrals. Here we take the simple case where $r_1 = r_2 = r_b$, r_b being the radius of the laser beam. We then get

$$L_S = \frac{16\, r_b}{3\pi \sin\Theta} \quad . \qquad (39)$$

Equation (39) does not apply to the scattering geometries where the scattering volume cannot be considered as the intersection volume of infinite identical cylinders such as extreme forward scattering, or where special selection optics are used. For the restrictive geometry considered we can set $\Theta = \delta_s$.

The number of photoelectrons, N_{pe}, is given by

$$N_{pe} = T_R q\, N_{ph} \qquad (40)$$

where T_R is the transmission factor of the collection optics and q is the quantum efficiency of the detector. The number of photoelectrons, N_f, for each partial interference fringe is then obtained from Eqns (35), (36), (39) and (40). On making the appropriate substitutions we obtain the approximate numerical expression

$$N_f \approx 300\, \frac{n_e\, B^2\, W\, \lambda_o^{\,3}\, r_b\, M^2\, T_R\, q}{T_e^{\frac{1}{2}} \sin\delta_s \sin\chi_s\, F} \qquad (41)$$

for the restrictive range of scattering geometries discussed in section 2.

4. CALCULATIONS FOR A TYPICAL SCATTERING EXPERIMENT

To illustrate the above theoretical and numerical results we choose a representative Tokamak plasma with T_e = 1 keV, $n_e = 2 \times 10^{19}$ m^{-3} and B_ϕ = 3 teslas. The appropriate scattering geometry is shown in Figures 1 and 3. A ruby laser beam (λ_o = 6943 Å) of pulse energy 10 joules and radius 5 mm is assumed. Typical collection optic parameters would be collection angle $\chi_s = 8^o$, optical transmission T_R = 25%, telescope magnification M = 10, and a quantum efficiency q = 6%. Setting B_θ/B_ϕ = 10%, and assuming that the laser beam is perpendicular to the poloidal field ($\beta = 90^o$) and the torus midplane we obtain for various collection cone inclination angles, δ_s, the parameter values listed in Table I. (The values given in this table were calculated from the exact expressions. In the δ_s = 0 column the scattering length was set equal to the one for $\delta_s = 30^o$). We can see immediately that the case for 90^o scattering offers the highest accuracy. Since the theoretical accuracy of 1% in determining the B_θ/B_ϕ value is more than sufficient, the laser beam divergence may be increased beyond 1.6 mrad. This is of advantage in achieving large incident laser beam energies and thus relaxing, somewhat, the photodetection problems.

However, scattering geometries with large values of δ_s have as a disadvantage a relatively wide scattered spectrum and hence a large number of peaks in the modulated spectrum. This increases the difficulty of accurately adjusting the interferometer mirror spacing to match the free spectral range to the peak spacing. As can be seen from Table I, a scattering angle, δ_s, of about 30^o offers the best compromise, in this case, for obtaining a large number of photoelectrons and high experimental accuracy, whilst, at the same time reducing the mismatch problem.

TABLE I

	δ_s^o	0^o	30^o	60^o	90^o
	μ_s^o	- 5.7	15.0	34.1	45.4
	$\Delta\mu_s^o$	.64	.68	.80	.92
	χ_{OMX} (mrad)	1.6	1.6	1.6	1.6
	$\Delta B_\theta - \Delta B_\phi\left(\frac{B_\theta}{B_\phi}\right)$ (T)	.034	.012	.006	.004
	$\Delta\left(\frac{B_\theta}{B_\phi}\right)$ (mrad)	11.2	4.4	2.5	2.2
F = 25	$\delta\Omega$ (μ ster)	35	37	25	25
	N_{pe}	25	26	18	18
F = 8	$\delta\Omega$ (μ ster)	108	115	78	78
	N_{pe}	77	82	55	55

Table I

Some important parameters for various scattering geometries on a representative Tokamak plasm of B_ϕ = 3T, B_θ = 0.3T, T_e = 1 keV and $n_e = 2 \times 10^{19}$ m^{-3}. A ruby laser of 10 J pulse energy is assumed.

5. CONCLUSIONS

The laser light scattering diagnostic, for measuring the magnetic field direction in a plasma, which was proposed by Sheffield, for a particular scattering geometry, has been presented in a general form to cover all scattering geometries and magnetic field configurations. It was then possible to study the effect that real experimental conditions would have, and to choose the scattering arrangement most suitable for the plasma in question. A representative Tokamak plasma of T_e = 1 keV, $n_e = 2 \times 10^{19}$ m^{-3}, B_{tor} = 3 T and B_{pol} = 0.3 T was considered where the laser beam was assumed to be parallel to the torus major axis. A low finesse Fabry-Perot interferometer with its mirror spacing adjusted to match the free spectral range to the spectrum peak spacing is assumed in the collection optics. The light intensity in the peaks is then superposed in the dispersed spectrum and so the whole spectrum of scattered light can be utilized. Large scattering angles yield higher accuracy in determining the field direction. For a ruby laser beam (λ_o = 6943 Å) with an energy of 10 Joules in the plasma and a beam divergence of about 2 mrad an experimental accuracy of 5% shall be feasible where about 80 useful photoelectrons are obtained with a scattering angle of 30^o.

ACKNOWLEDGEMENTS

I wish to thank H A B Bodin, D E Evans, M J Forrest, J Katzenstein, N J Peacock and J Sheffield of Culham Laboratory for many helpful discussions. The encouragement given by F Waelbroeck while I was at the Institut für Plasmaphysik, Jülich to complete this work is kindly appreciated.

REFERENCES

Born M. and Wolf E. (1959) 'Principles of Optics' pp322-330, Pergamon Press, London.

Carolan P.G. and Evans D.E. (1971a) Plasma Phys. 13, 947.

Carolan P.G. and Evans D.E. (1971b) 10th Int.Conf.Phenom.Ion.Gases, Oxford P413.

Evans D.E. and Carolan P.G. (1970) Phys.Rev.Lett. 25, 1605.

Jacquinot J. (1954) J.Opt.Soc.Am. 44 10, 761.

Katzenstein J. (1972) Culham Laboratory, private communication.

Kellerer L. (1970) Z.Physik 232, 415.

Ludwig D. and Mahn C. (1971) 10th Int.Conf.Phenom.Ion.Gases, Oxford P416.

Meyer R.L. and Leclert G. (1972) Nuclear Fusion 12, 269.

Murakami M. and Clarke J.F. (1971) Nuclear Fusion 11, 147.

Perkins F.W. (1970) Princeton Plasma Physics Laboratory, MATT 818.

Sheffield J. (1972) Plasma Phys. 14, 385.

APPENDIX

A1. THE WAVE VECTORS $\vec{k}_o$, $\vec{k}_s$ AND $\vec{k}$ FOR AN ARBITRARY SCATTERING GEOMETRY

In a successful experiment the raw data available to the experimentalist will be the angular coordinates of two partial interference fringes at the focal plane of a Fabry-Perot or a Michelson placed in the scattered light collection optics. The two fringes readily give the angular conical coordinates of the scattered light directions which exhibit magnetic modulation. But before the magnetic field direction can be calculated from these coordinates it is necessary to transform all relevant vectors to a common coordinate system (viz x,y,z system of Figure 2(b)).

In Figure A1 the orientation of an arbitrary laser beam axial direction, OL, is shown in relation to the x,y,z coordinate system (cf. section 2) where

δ_o is the angle between OL and the y axis

ξ_o is the angle between the plane OL, y and the xy plane.

A coordinate system x_o, y_o, z_o, convenient for the input optics, is obtained from the x,y,z coordinate system by a rotation of ξ_o about the y axis, giving the x', y', z' system, and then by a rotation of δ_o about the z' axis (cf. Figure A1). A wave vector $\vec{k}_o$ expressed in the x_o, y_o, z_o system can then be easily transformed into its x,y,z components.

Similarly, another coordinate system x_s, y_s, z_s, is defined for the collection cone with the corresponding angles δ_s and ξ_s where

δ_s is the angle between OS and the y axis

ξ_s is the angle between the plane OS, y and the xy plane.

We now have

$$\begin{pmatrix} x \\ y \\ z \end{pmatrix} = \begin{pmatrix} \cos\xi_o & 0 & \sin\xi_o \\ 0 & 1 & 0 \\ -\sin\xi_o & 0 & \cos\xi_o \end{pmatrix} \begin{pmatrix} x' \\ y' \\ z' \end{pmatrix} = A_o \begin{pmatrix} x' \\ y' \\ z' \end{pmatrix} \qquad \text{(A1)}$$

and

$$\begin{pmatrix} x' \\ y' \\ z' \end{pmatrix} = \begin{pmatrix} \cos\delta_o & -\sin\delta_o & 0 \\ \sin\delta_o & \cos\delta_o & 0 \\ 0 & 0 & 1 \end{pmatrix} \begin{pmatrix} x_o \\ y_o \\ z_o \end{pmatrix} = A'_o \begin{pmatrix} x_o \\ y_o \\ z_o \end{pmatrix} \qquad \text{(A2)}$$

.

From Eqns. (A1) and (A2) we have

$$\begin{pmatrix} x \\ y \\ z \end{pmatrix} = A_o A_o' \begin{pmatrix} x_o \\ y_o \\ z_o \end{pmatrix} \tag{A3}$$

Similarly, we have

$$\begin{pmatrix} x \\ y \\ z \end{pmatrix} = A_s A_s' \begin{pmatrix} x_s \\ y_s \\ z_s \end{pmatrix} \tag{A4}$$

It now remains to express a particular $\vec{k}_o$ and $\vec{k}_s$ in the x_o, y_o, z_o and x_s, y_s, z_s systems respectively and then perform the transformations of Eqns. (A3) and (A4) to express the vectors in the x,y,z system. Figure A.2 shows the angles necessary to define a particular $\vec{k}_o$ and $\vec{k}_s$ where

χ_o/χ_s is the angle between $\vec{k}_o/\vec{k}_s$ and OL/OS

μ_o/μ_s is the angle between the plane OL,y/OS,y and the plane defined by OL/OS and $\vec{k}_o/\vec{k}_s$

θ is the angle between $\vec{k}_o$ and $\vec{k}_s$

γ_o/γ_s is the laser cone/collected cone apex angle.

Then expressing $\vec{k}_o$ and $\vec{k}_s$ in the x_o, y_o, z_o and x_s, y_s, z_s systems we have

$$\vec{k}_o = k_o \begin{pmatrix} \sin\chi_o \cos\mu_o \\ \cos\chi_o \\ -\sin\chi_o \sin\mu_o \end{pmatrix}_{x_o,\, y_o,\, z_o} \tag{A5}$$

and

$$\vec{k}_s = k_o \begin{pmatrix} \sin\chi_s \cos\mu_s \\ \cos\chi_s \\ -\sin\chi_s \sin\mu_s \end{pmatrix}_{x_s,\, y_s,\, z_s} \tag{A6}$$

where it is assumed that $k_s = k_o$ for small Doppler shifts.

Therefore, from Eqns. (A3) and (A4) we have

$$\vec{k}_o = k_o \left(A_o A_o' \begin{pmatrix} \sin \chi_o \cos \mu_o \\ \cos \chi_o \\ -\sin \chi_o \sin \mu_o \end{pmatrix} \right)_{x,y,z} \qquad \text{(A7)}$$

and

$$\vec{k}_s = k_o \left(A_s A_s' \begin{pmatrix} \sin \chi_s \cos \mu_s \\ \cos \chi_s \\ -\sin \chi_s \sin \mu_s \end{pmatrix} \right)_{x,y,z} \qquad \text{(A8)}$$

The scattering wave vector $\vec{k} = \vec{k}_s - \vec{k}_o$ can then be easily obtained from Eqns. (A7) and (A8).

A2. AZIMUTHAL HALF WIDTH, $\Delta\mu_s$, FOR WHICH MAGNETIC MODULATION WILL BE OBSERVED

We have from Eqn. (10)

$$\Delta\mu_s \approx \frac{B\omega_{ce}}{2v_e} \left[\frac{\partial}{\partial \mu_s} f_{al}(\mu_s') \right]^{-1} . \qquad \text{(A9)}$$

We can then write for the derivative in Eqn. (A9)

$$\begin{aligned} \frac{\partial}{\partial \mu_s} f_{al}(\mu_s') &= \vec{B} . \frac{\partial}{\partial \mu_s} \vec{k} \\ &= \vec{B} . \frac{\partial}{\partial \mu_s} \vec{k}_s \\ &= - B_\theta \sin\beta \, k_{sx}' + B_\theta \cos\beta \, k_{sy}' + B_\phi \, k_{sz}' . \end{aligned} \qquad \text{(A10)}$$

The derivatives k_{sx}', k_{sy}' and k_{sz}' are obtained from Eqn. (A8). On substituting we get

$$\frac{\partial}{\partial \mu_s} f_{al}(\mu_s') = k_o \sin \chi_s . B_\phi . g_s \qquad \text{(A11)}$$

where

$$\begin{aligned} g_s = \frac{B_\theta}{B_\phi} \Big[&\left(\cos\xi_s \cos\delta_s \sin\mu_s' + \sin\xi_s \cos\mu_s' \right) \sin\beta - \sin\delta_s \sin\mu_s' \cos\beta \Big] \\ &+ \Big[\sin\xi_s \cos\delta_s \sin\mu_s' - \cos\xi_s \cos\mu_s' \Big] . \end{aligned} \qquad \text{(A12)}$$

On combining Eqns. (A9) and (A11), we obtain Eqn. (11). (For the most relevant cases where $\delta_o = \xi_o = \gamma_o = \xi_s = 0$ and $\beta = 90^o$ the factor g_s is not very dependent on B_θ/B_ϕ or δ_s values and can be approximated by $g_s \approx 1$, provided $B_\theta/B_\phi \sin\delta_s \ll \tan\chi_s$).

A3. LASER BEAM DIVERGENCE

Suppose, for a particular scattered wave vector, $\vec{k}_s$, and where the incident wave vector $\vec{k}_o$ is along the laser beam axis, that we have

$$f_{al}\ (\vec{k}_o) = \vec{k}.\vec{B} = 0 \quad . \tag{A13}$$

We now wish to determine the maximum value, χ_{OMX}, of conical apex angle that will not contain an incident wave vector, $\vec{k}_o'$, for which the corresponding scattering wave vector $\vec{k}'$ satisfies

$$\vec{k}'.\vec{B} = \frac{B\omega_{ce}}{2v_e} \quad . \tag{A14}$$

As we require only an approximate value of χ_{OMX} we limit the analysis by setting $\delta_o = \xi_o = \xi_s = 0$ and $\beta = 90^o$. Since the wave vector $\vec{k}_s$ is held constant, we get from Eqns. (A13) and (A14)

$$\frac{B\omega_{ce}}{2v_e} = (\vec{k}_o' - \vec{k}_o).\vec{B} \quad . \tag{A15}$$

We also get from Eqn. (A7)

$$\vec{k}_o' - \vec{k}_o = k_o \begin{pmatrix} \sin \chi_{OMX} \cos \mu_o \\ \cos \chi_{OMX} - 1 \\ - \sin \chi_{OMX} \sin \mu_o \end{pmatrix} \quad . \tag{A16}$$

It can then be easily shown that

$$\chi_{OMX} = \sin^{-1} \left\{ \frac{B\omega_{ce}}{2(B_\phi \sin \mu_o + B_\theta \cos \mu_o)\ k_o\ v_e} \right\} . \tag{A17}$$

In the case where $B_\phi >> B_\theta$ and $\omega_{ce} << 2k_o v_e$ we obtain

$$\chi_{OMX} = \frac{\omega_{ce}}{2k_o v_e} \quad . \tag{A18}$$

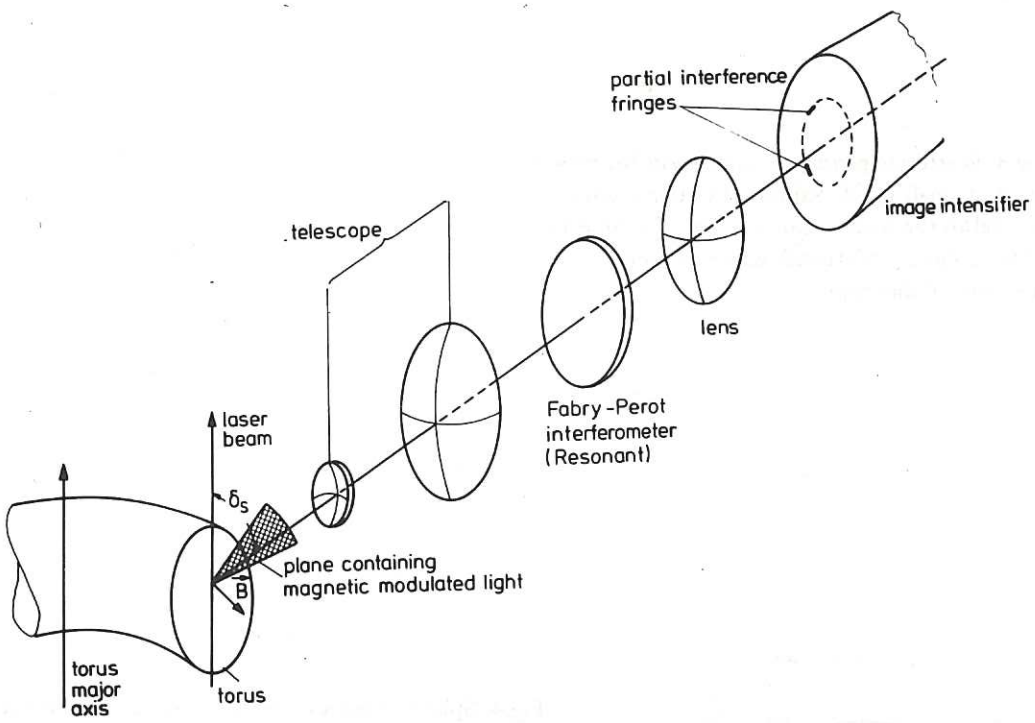

Fig.1 Optical arrangement for the measurement of the magnetic field direction in a Tokamak plasma.

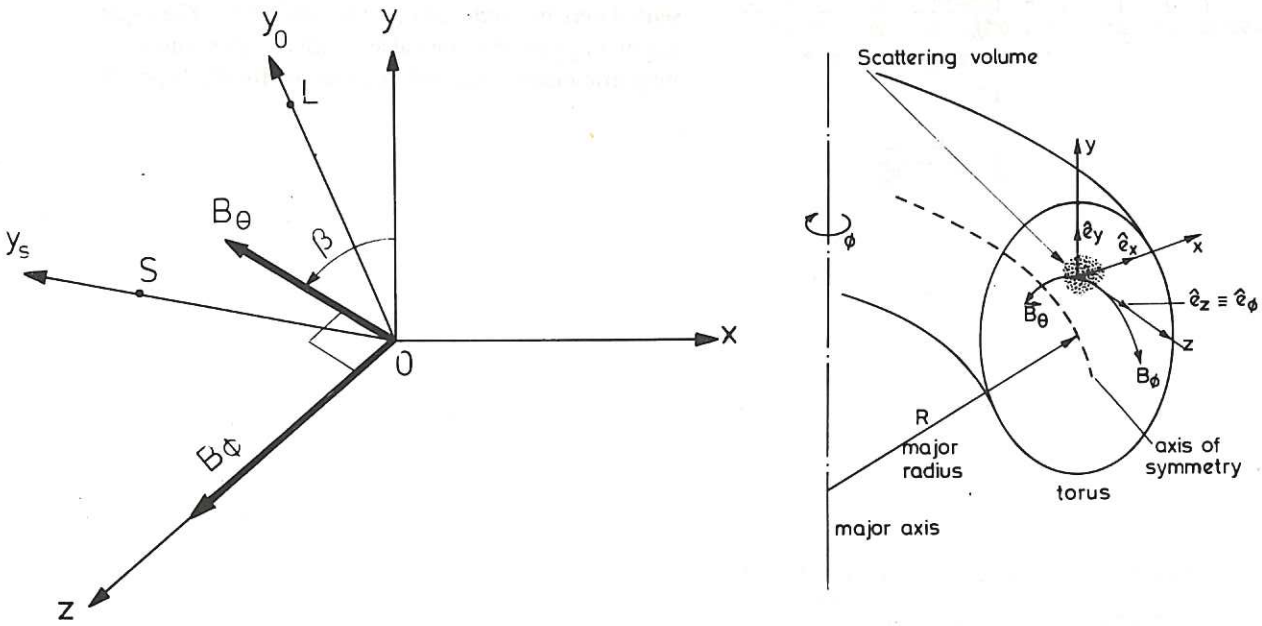

Fig.2 Relation of the x,y,z coordinate system to the toroidal and poloidal fields $\vec{B}_\phi$ and $\vec{B}_\theta$. OL and OS are the axes of the incident laser beam and the collected cone of scattered light respectively.

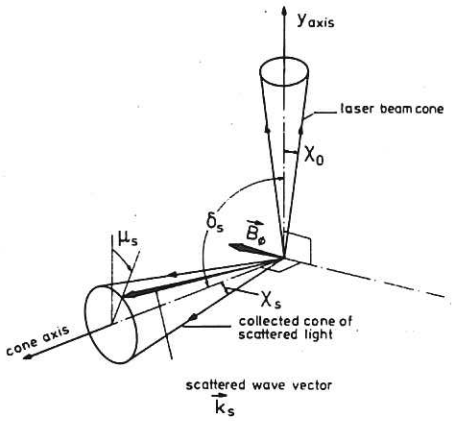

Fig.3 Scattering geometry convenient for measurement of small B_θ/B_ϕ values. The laser beam is parallel to the torus major axis and the cone axis of the collected scattered light is perpendicular to the toroidal direction.

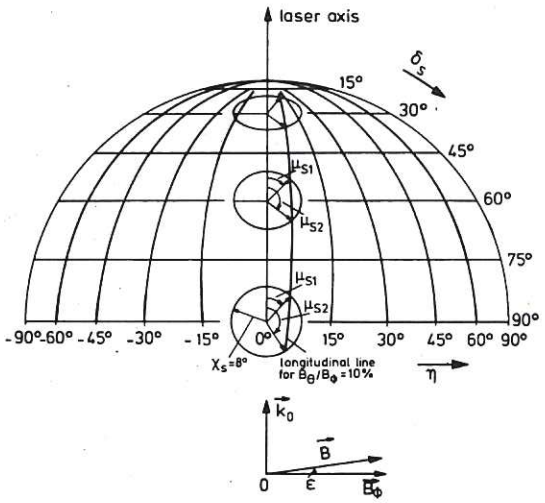

Fig.4 Spherical representation of scattered wave vectors. The scattering volume is at the sphere centre. The axis of the sphere is the laser beam which is considered to be perpendicular to both $\vec{B}_\phi$ and $\vec{B}_\theta$. The plane perpendicular to $\vec{B}$, containing the modulated scattered light, intersects the sphere surface along a line of longitude $n = \epsilon$ where ϵ is the angle between $\vec{B}$ and $\vec{B}_\phi$. Collected cones of scattered wave vectors are represented here by circles at $\delta_s = 90°, 60°, 30°$. The angles μ_{s1} and μ_{s2} are the conical azimuthal angles where magnetic modulation will be observed for $B_\theta/B_\phi = 10\%$.

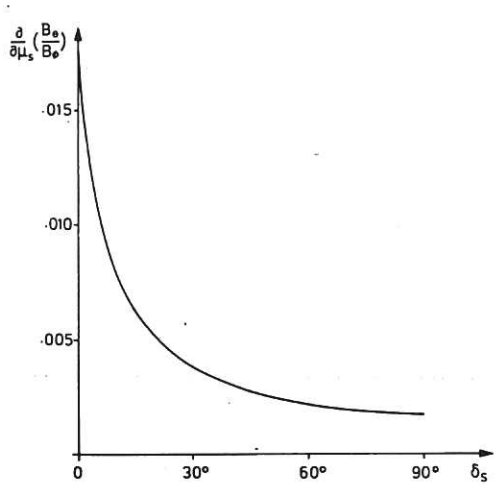

Fig.5 Variation of the derivative $\frac{\partial}{\partial \mu_s}(B_\theta/B_\phi)$ as a function of δ_s for $B_\theta/B_\phi = 10\%$.

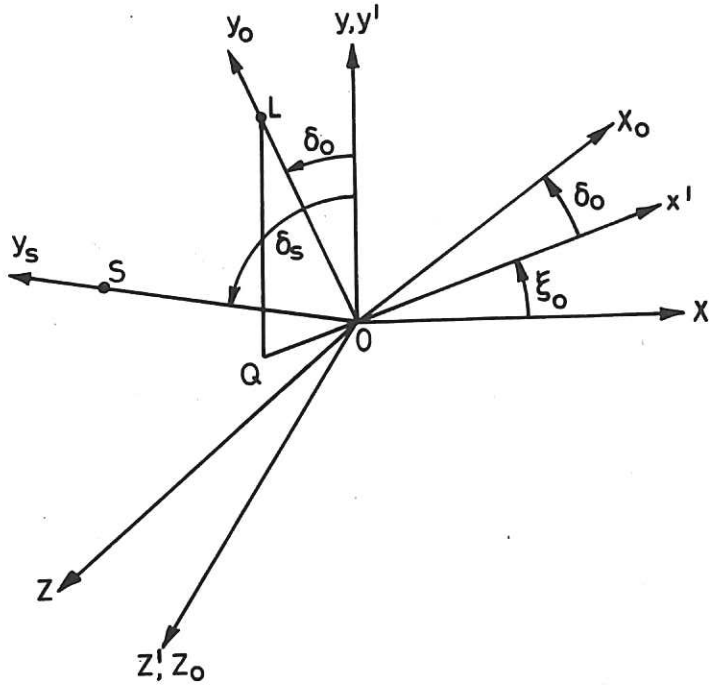

Fig.A.1 Relation of the x_o, y_o, z_o coordinate system of the laser beam to the basic x,y,z coordinate system.

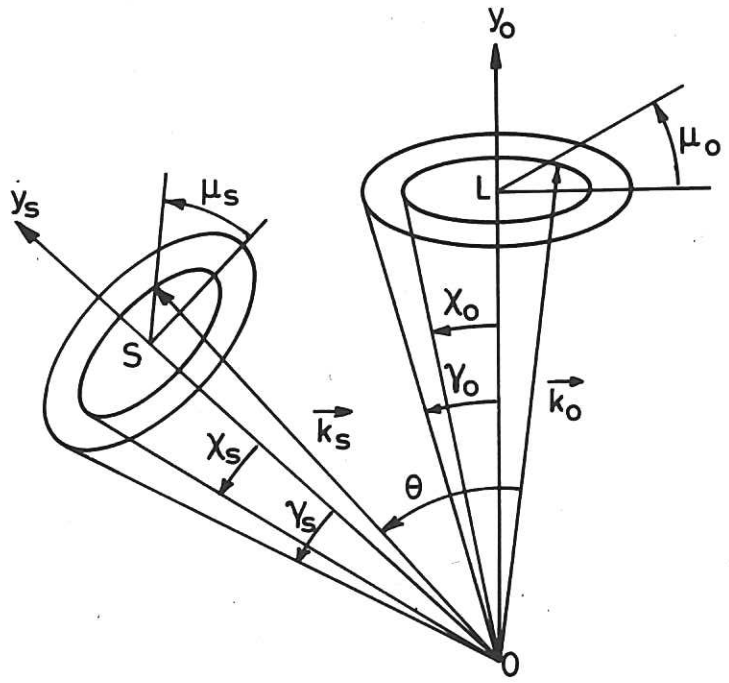

Fig.A.2 Conical coordinate systems for the incident laser beam and the collected cone of scattered light.